

Decomposition of Chemical Warfare Agent Simulants

Utilizing Pyrolyzed Cotton Balls as Wicks

Bryan A. Lagasse,^{1,2} Laura McCann,¹ Timothy Kidwell,³ Matthew S. Blais,^{3*} and Carlos D Garcia^{1*}

¹*Department of Chemistry, Clemson University, 211 S. Palmetto Blvd., Clemson, SC 29634*

²*Department of Chemistry and Life Science, United States Military Academy, West Point, NY 10996*

³*Southwest Research Institute, 6220 Culebra Road, San Antonio, TX 78238*

Alternative routes for the fabrication of carbon wicks. In the event that a tube furnace (high temperature, oxygen-free atmosphere) is not available, the following procedures can be used make 3D wicks that could potentially be used for this purpose:

- <https://graywolfsurvival.com/3002/make-use-char-cloth/>
- <https://survival-training.wonderhowto.com/how-to/make-fire-starting-char-cloth-from-t-shirt-using-tuna-can-0143975/>

These links were last verified/accessed on July 10, 2020

Alternative views of the experimental set-up, to show the location of the CaCO_3 shield



Figure S1: Alternative views of the experimental set-up for the burning of chemical warfare agent simulants while measuring overflow, where the CaCO_3 shield is more visible.

Scanning electron microscope image of non-pyrolyzed cotton ball fibers and pyrolyzed cotton ball fibers. As shown in Figure S2, there is a significant change in the 3-dimensional structure of the individual cellulose fibers as a result of the pyrolysis process. This is believed to both increase the surface area of the individual fibers and contribute to the changes in the hydrophobicity of the resulting cellulose fibers. It is posited that these structural changes contribute to the increased rate of maximum burning which was observed when pyrolyzed cotton balls serve as the substrate for the incendiary agent

as compared to the unpyrolyzed cotton balls. The pyrolyzation process not only causes a loss of 95% of the cotton ball's mass, but it also reduces its size by over 50%. As shown by Figure S2 the individual cellulose fibers undergo a drastic change in structure, from a mostly flat and folded fiber, to a helical and twisted fiber. This indicates there are significant changes to the fiber's molecular structure.

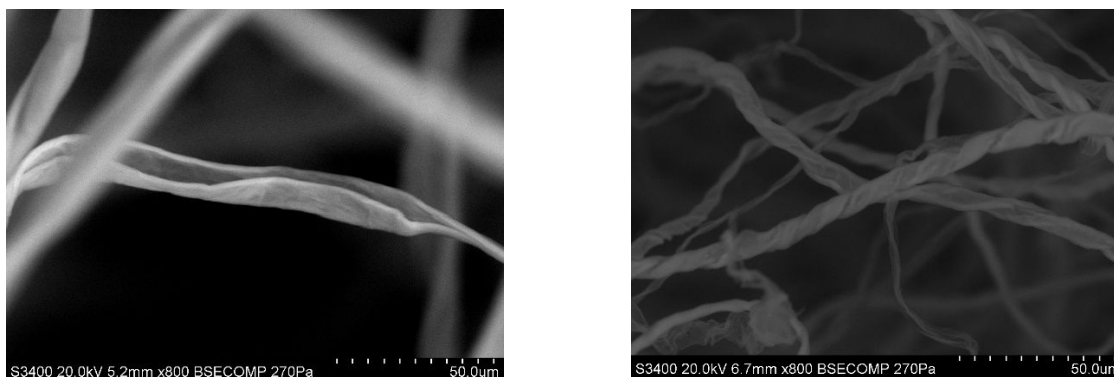


Figure S2: Scanning electron microscope image of non-pyrolyzed cotton ball fibers (left) and pyrolyzed cotton ball fibers (right) displaying the change in the 3-dimensional structure of the individual fibers as a result of the pyrolyzing process.

Optical Profilometry. The optical non-contact roughness measurements of the interior and exterior surfaces of the pyrolyzed cotton balls revealed there was a consistent structure throughout the pyrolyzed cotton balls. The average fiber diameter for both interior and exterior fibers was calculated at $9.70 \pm 1.23 \mu\text{m}$. Similarly, the roughness measurements of both interior and exterior portions of the cotton balls were consistent throughout the cotton balls. This supported the hypothesis that the pyrolyzation process resulted in a homogeneous change to the cellulose fibers of the cotton ball. Furthermore, this supported the hypothesis that the change in size of the cotton ball was due to the coalescing of the fibers to form more an intertwined fiber network with smaller voids. As the voids between fibers appear to have decreased in size following pyrolysis suggests the ability of the pyrolyzed fibers to both support the napalm mixture and wick the liquid agent towards the flame without absorbing the agent are critical in the ability to achieve thermal decomposition.

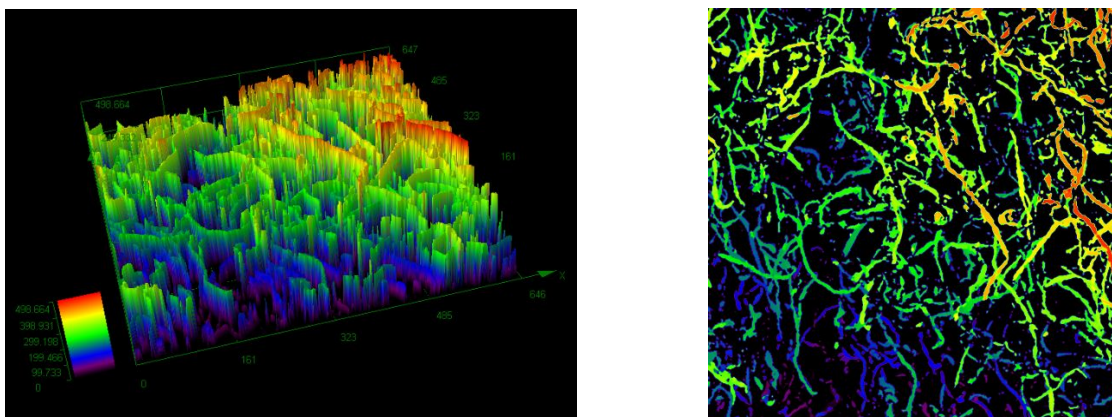


Figure S3: Optical non-contact roughness measurements of interior structure of pyrolyzed cotton ball: (left) three dimensional rendering of the imaged area of the pyrolyzed cotton ball displaying the varied height of the fiber in reference to the objective; (right) superimposed height image on the two dimensional image of pyrolyzed cotton ball

Nitrogen adsorption isotherms. The linear isotherm in both the adsorption and desorption of $N_2(g)$ demonstrates that the pyrolyzed cotton balls are relatively uniform in composition. By the BET method, the surface area of the pyrolyzed cotton balls was determined to be $569.624 \text{ m}^2/\text{g}$.

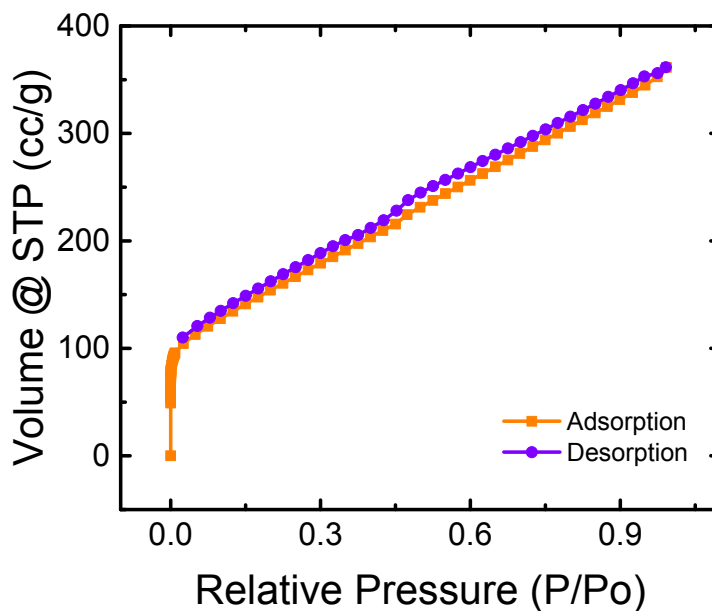


Figure S4: BET isotherm for pyrolyzed cotton balls indicating that there is a linear adsorption and desorption of nitrogen gas yielding a total surface area of $569.624 \text{ m}^2/\text{g}$

The pore size distribution by the BJH method shows the majority of pores are approximately 19 Å in size. These small pores lend to the pyrolyzed cotton fibers serving as a wick for the incendiary agent. When compared to mesoporous carbon surfaces the pyrolyzed cotton balls exhibit a slightly lower overall surface area and significantly smaller pores.¹

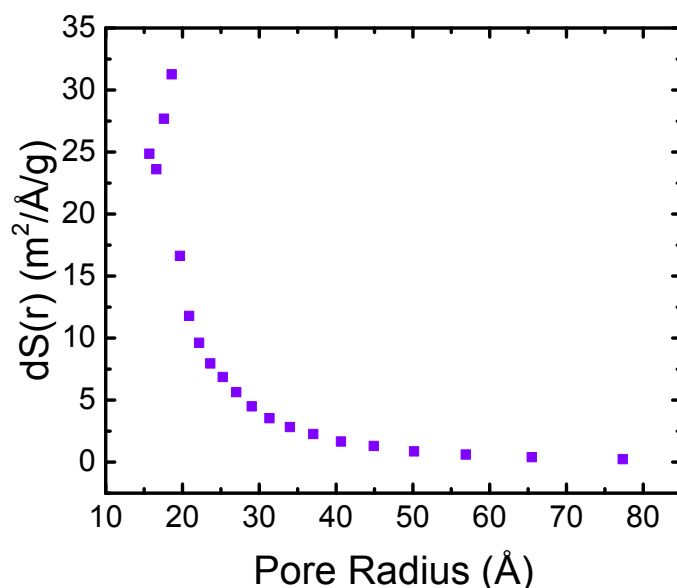


Figure S5: Pore size distribution in pyrolyzed cotton balls by the BJH method showing the majority of pores' radius are centered around the 19 Å

Hydrophobicity. In order to demonstrate the hydrophobic qualities of the pyrolyzed cotton balls a rudimentary contact angle assessment was conducted. In this study both unpyrolyzed and pyrolyzed cotton balls were placed in a dish and had a small quantity of water pipetted onto the surface. As expected, the unpyrolyzed cotton balls rapidly absorbed the water as soon as the water droplet contacted the fibers due to the hydrophilic properties of cellulose. The pyrolyzed cotton balls however, did not absorb the water (Figure S6). This arrangement was observed for 5 minutes with no discernable change. While it was not possible to determine the contact angle between the water droplet and the individual pyrolyzed cotton ball fibers using this experiment, it demonstrated that the pyrolyzation process converts the cellulose fibers into non-polar carbonized fibers which are highly hydrophobic. To reinforce this assessment both unpyrolyzed and pyrolyzed cotton balls were individually suspended and slowly

lowered into a watch glass filled with water. When the unpyrolyzed cotton ball fibers made contact with the surface of the water, the water began to wick up through the fibers into the bulk mass of the cotton ball.



Figure S6: Image of pyrolyzed cotton ball with a drop of water supported on the surface due to the hydrophobic interaction between the pyrolyzed cotton ball fibers and the water droplet.

This hydrophilic interaction was strong enough that even when the cotton ball was slightly retracted from the surface of the water, the wicking continued until the cotton ball was fully saturated (Figure S7).

Conversely, when the pyrolyzed cotton ball was lowered to the surface of the water no wicking occurred and the pyrolyzed cotton ball was suspended on the surface of the water.

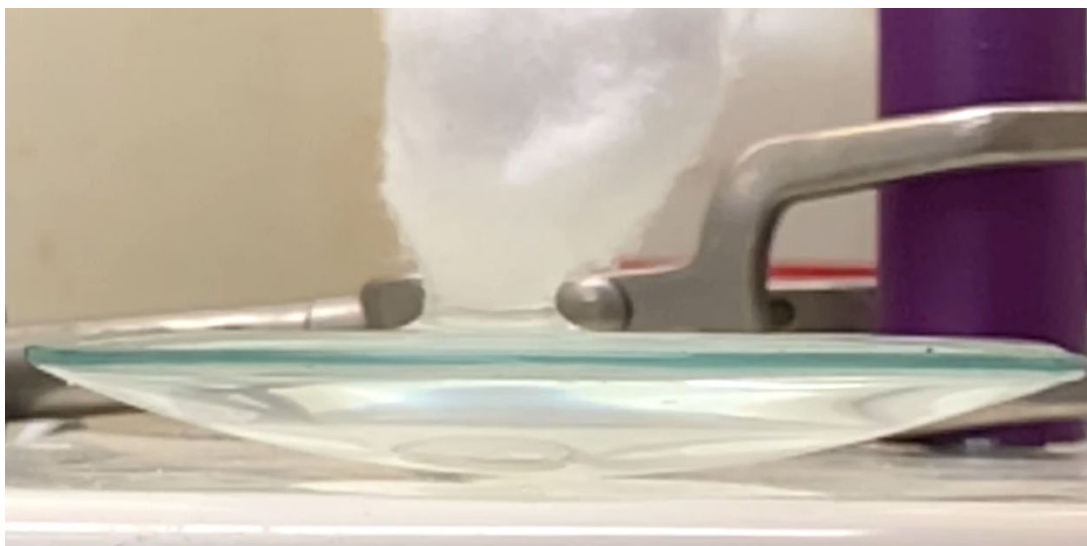


Figure S7: Image of the results of the hydrophilic interaction between unpyrolyzed cotton ball fibers and water as the cotton ball was slowly retracted from the surface of the water, but continued wicking the water into the bulk of the cotton ball mass.

Evaporation and Degradation. The FTIR spectra taken from samples where degradation occurred with a pool of liquid CEES at room temperature, 50 °C, and 80 °C (Figure S8). The peaks were compared to literature values, confirming that they aligned with CEES products. Measurements of CEES concentration in the vapors was made using the peak at 2888.39 cm^{-1} , as the HCl peak, another major by-product of CEES degradation, masking the other peaks during combustion.

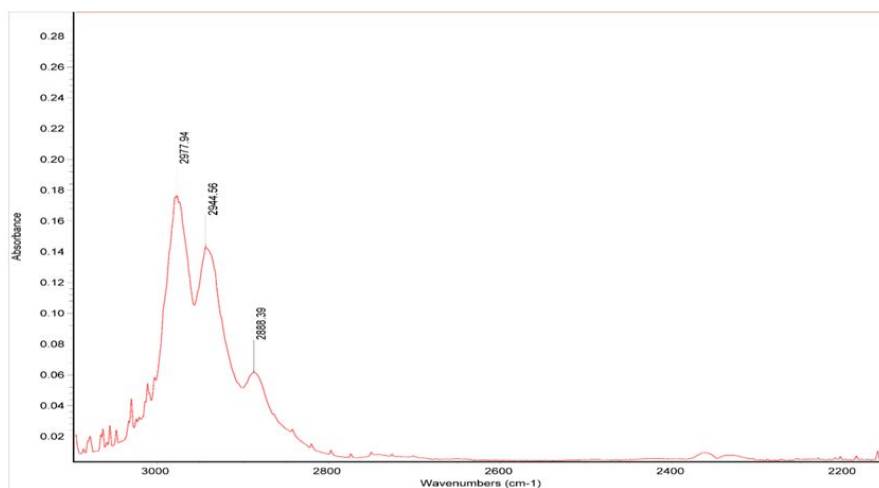


Figure S8: FTIR spectrum of CEES vapor from experiments conducted below 80 °C. The peaks are labelled corresponding to their location on the CEES molecule. The peak at 2888.39 cm^{-1} was used to measure CEES vapor concentration.

By measuring the concentration of CEES in the emitted vapors across the time scale course of the experiment (Figure S9) it was demonstrated that when the pool of CEES is ignited a sharp increase in the concentration of CEES in the gaseous phase occurs, however this concentration rapidly decreases as the temperature of the pool increases and the simulant begins to decompose through a pericyclic reaction.

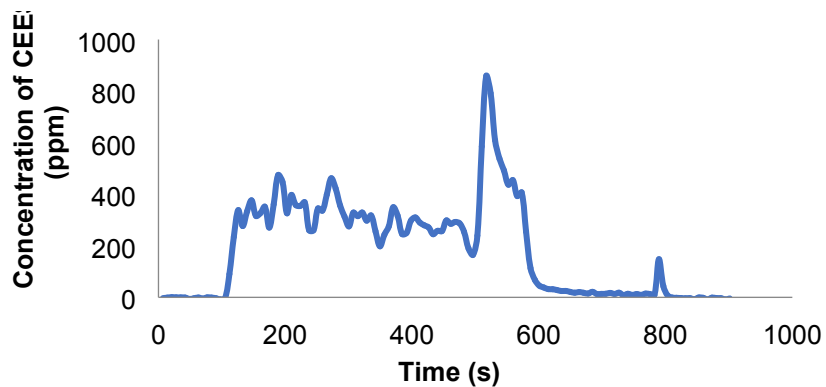


Figure S9: Concentration of CEES in gas phase over time. At 484 s, the pool was ignited. At 535 s, the pool was extinguished. At 782 s, purge air was flushed through the system.